

# Simulations of Atmospheric General Circulations of Earth-like Planets by AFES

Project Representative

Yoshi-Yuki Hayashi      Department of Earth and Planetary Sciences, Kobe University

Authors

Yoshi-Yuki Hayashi      Department of Earth and Planetary Sciences, Kobe University

Yoshiyuki O. Takahashi      Department of Earth and Planetary Sciences, Kobe University

Norihiko Sugimoto      Research and Education Center for Natural Sciences, Keio University

Masahiro Takagi      Faculty of Science, Kyoto Sangyo University

Hiroki Kashimura      Project Team for Risk Information on Climate Change, Japan Agency for Marine Earth  
Science and Technology

Masaki Ishiwatari      Department of CosmoSciences, Hokkaido University

Masatsugu Odaka      Department of CosmoSciences, Hokkaido University

Kensuke Nakajima      Department of Earth and Planetary Sciences, Kyushu University

George L. Hashimoto      Department of Earth Sciences, Okayama University

Yoshihisa Matsuda      Faculty of Education, Tokyo Gakugei University

High resolution simulations of the Venus and Mars atmospheres have been performed by using a General Circulation Model (GCM) based on AFES (Atmospheric GCM for the Earth Simulator). Our aim is to have insights into the dynamical features of small and medium scale disturbances in the Earth-like atmospheres and their roles in the general circulations. As for the simulation of the Venus atmosphere, a superrotation consistent with observations is reasonably reproduced with a realistic solar heating. Baroclinic waves appear in a weakly stratified layer with large vertical shear of the basic zonal flow at the cloud level. Rossby and Kelvin waves generated in the model are consistent with observations. They transport momentum and heat. Furthermore, a realistic polar cold collar, which is a cold band zonally surrounding the polar vortex, is reproduced in the polar region. The structure is closely related to residual mean meridional circulation enhanced by thermal tides. In the results with a high-resolution simulation (T159L120), spectral analyses of the horizontal kinetic energy show that small-scale gravity waves might be more important in Venus than in Earth. The present results indicate that the realistic vertical distribution of static stability with thermal tides and sufficient model resolution are crucial for reproducing the structure of the Venus atmosphere. As for the simulation of the Martian atmosphere, some nature of small scale vortices observed in high resolution simulations are examined by performing additional experiments with a convective adjustment. Those small scale vortices in the low latitudes are one of the most prominent features in our high resolution simulations. However, since they appear at around the limit of the model horizontal resolution, it was not clear how robust they are, and it may depend on the details of parameterization implemented in the model. A simulation with convective adjustment shows that small scale vortices are still generated, although its strength is decreased slightly. Additional experiments with uniform surface properties, orography, surface albedo and surface thermal inertia, show that vorticity appears more like a filament structure rather than a lot of vortices. These results imply that the existence of small scale vortices does not depend on details of parameterization in the model. In addition, it is also shown that those vortices are generated from filament structure destroyed by orography-related disturbances.

**Keywords:** planetary atmospheres, superrotation, dust storm, Earth, Mars, Venus

## 1. Introduction

The structure of the general circulation differs significantly in each of the planetary atmospheres. For instance, the atmospheres of the slowly rotating Venus and Titan exemplify the states of superrotation where the equatorial atmospheres rotate faster than the solid planets beneath, while the equatorial easterly and the strong mid-latitude westerly jets form in the

Earth's troposphere. The global dust storm occurs in some years on Mars, while a similar storm does not exist in the Earth's atmosphere. Understanding physical mechanisms causing such a variety of features in the general circulations of the planetary atmospheres is one of the most interesting and important open questions of the atmospheric science and fluid dynamics.

The aim of this study is to understand dynamical processes

that characterize the structure of each planetary atmosphere by performing simulations of those planetary atmospheres by using GCMs with a common dynamical core of AFES [1]. Appropriate physical processes are adopted for each planetary atmosphere. In the followings, the particular targets of each simulation, the physical processes utilized, and the results obtained will be described briefly.

## 2. Venus simulation

### 2.1 Targets of simulations

In the past two decades, low-resolution GCMs have been used to simulate phenomena in the Venus atmosphere (e.g., [2]). This is mainly because of the extremely long spin-up time to generate a superrotation from a motionless state. Furthermore, in order to generate a superrotation, most of the previous GCM studies have included unrealistic strong solar heating and static stability. In the present study, we have been constructing a new model based on AFES to perform realistic high-resolution simulations of the Venus atmosphere.

Many observational studies have reported signals of planetary-scale Rossby- and Kelvin-type waves at the cloud top, which propagate faster and slower than the zonal flow, respectively (e.g., [3,4]). However, the waves obtained in the previous numerical studies are not consistent with observations (e.g., [5]). This is partly because the fast mean zonal flow has not been reproduced realistically in the models. Further, the weakly stratified layer in the cloud layer has been neglected in their models. At the polar region, the polar cold collar, a cold band zonally surrounding the polar vortex, is a unique feature observed at the ~65 km level [6]. However, there have been no numerical simulations which reproduce a realistic distribution of the cold collar so far. Furthermore, observational studies [7] suggest that small-scale gravity waves play important roles at the cloud level. Although kinetic energy spectra have been utilized to explore properties of disturbances of a wide range of scales both in observational and numerical studies of the Earth atmosphere [8,9], those of the Venus atmosphere have not been well described yet.

AFES for Venus with a realistic solar heating and static stability has successfully reproduced a superrotation consistent with the observations. In this fiscal year, we perform simulations with very high resolutions to investigate properties of disturbances in a wide range of scales in the Venus atmosphere. The neutral waves and the polar cold collar are also important targets to take advantage of a high resolution model.

### 2.2 Model and experimental settings

Venus simulations are performed with simplified physical processes adopting the values of physical constants appropriate for Venus. The experimental settings basically follow those of the previous AFES simulations [10,11]. The highest resolution used in the present simulations is T159L120, which is

equivalent to a horizontal grid size of about 79 km. The vertical domain extends from the ground to about 120 km with almost the constant grid spacing of 1 km. Simulations with T63L120 and T42L60 resolutions, which are equivalent to horizontal grid sizes of about 198 and 297 km with 120 and 60 vertical layers, respectively, are also performed.

The physical processes adopted in the model are vertical eddy diffusion with a constant diffusion coefficient of  $0.15 \text{ m}^2/\text{s}$ , the Newtonian cooling, and the Rayleigh friction at the lowest level representing the surface friction. In the upper region above about 80 km, a sponge layer is assumed; the friction increasing gradually with altitude acts to damp the eddy component only. In addition, the model includes a 4th-order horizontal diffusion ( $\nabla^4$ ) with an e-folding time for the maximum wavenumber of about 0.01 days for T159, 0.03 days for T63, and 0.1 days for T42 simulations. The coefficients of the Newtonian cooling are based on the previous study [12]. The equilibrium temperature distribution toward which temperature is relaxed by the Newtonian cooling is the prescribed horizontally uniform temperature distribution based on observations. We adopt a realistic profile of solar heating. Vertical and horizontal distributions of the solar heating are based on Tomasko et al. [13].

The vertical temperature profiles of the initial conditions are constructed based on the observed vertical distribution of static stability [14]. In this temperature profile, the lower atmosphere near the ground is weakly stable. Below the cloud layer, static stability has a maximum at around 45 km. A layer with almost neutral stability exists from 55 to 60 km representing the cloud layer influenced by solar heating. Above the cloud layer (above 70 km), it is strongly stratified. Meridional temperature gradient from equator to pole is about 5 K on the model level, i.e., constant sigma surface, at the top of the cloud layer. The initial condition for wind velocity is zonally symmetric, solid-body superrotating flow, which is determined by the gradient wind balance; zonal velocity at the equator linearly increases from zero at the ground up to 100 m/s at the altitude of 70 km, and above there the atmosphere is in a solid-body rotation with the same speed as that at 70 km. From this initial condition, time integration is performed for four Earth years for T159 and T42 simulations. In addition, for the investigation of neutral waves, we perform time integration for ten Earth years for T63 simulation.

### 2.3 Results

Starting from the idealized superrotation, the model atmosphere reaches a quasi-equilibrium state within one Earth year. The wind and temperature fields are stably maintained for more than four Earth years for all simulations. The zonal-mean zonal flow, which is accompanied with weak mid-latitude jets, has almost constant velocity of 120 m/s in latitudes between 45°S and 45°N at the cloud top levels. This meridional

distribution of the zonal flow agrees very well with observations (e.g., [5]). Strong latitudinal temperature gradient is produced at 45–70 km, where the temperature difference between the equator and the pole is more than 25 K. Strong baroclinicity, i.e., large vertical shear of the zonal flow is maintained at mid-latitudes in the weakly stratified layer extending from 50 to 70 km by the solar heating.

The horizontal structure of the baroclinic waves observed at 70 km for T63 simulation is shown in Fig. 1a. In mid-latitudes between 30° and 60° the zonal wave number 1 component of geopotential height is predominant. These disturbances are in phase with temperature deviations at the altitude of 60 km (color). The result suggests that so-called Rossby waves observed at the cloud top are generated by the baroclinic waves excited at around the altitude of 60 km. The period of the waves is about 5.8 days. The phase speed of about 76 m/s is slower than the mean zonal flow of about 120 m/s at the height of 70 km. These wave characteristics are in good agreement with the observed so-called Rossby waves [4]. It is noted that the horizontal structure is reminiscent of the Y shape observed in UV images of Venus [3]. Below the altitude of 50 km, planetary-scale waves with zonal wave number 1 appear in the low latitudes between 30°S and 30°N, where zonal winds are predominant (Fig. 1b). The horizontal structure of the equatorial waves is similar to the so-called Kelvin waves. The period of the equatorial waves is about 6.2 days which is consistent with those observed at the levels of 50–60 km [15]. The phase velocity of the equatorial waves is about 70 m/s. The equatorial waves propagate faster and slower than the zonal-mean zonal flow velocity of the equatorial region below and above this level, respectively. These results are summarized in [16].

The time evolution of the horizontal temperature distribution at the altitude of 68 km for T42 simulation is shown in Fig. 2.

The cold collar surrounds the warmer polar region at around 60°N. The maximum temperature difference between 60°N and the pole is about 20 K. The hot polar region rotates around the pole, and changes its shape temporally, showing an S-shaped structure (Fig. 2b) occasionally. These features are in a close agreement with the cold collar and the polar vortex observed in optical measurements (e.g., [6]). Further analysis explains that the structure is closely related to residual mean meridional circulation enhanced by thermal tides; the cold collar is not reproduced when thermal tides are removed by omitting a diurnal component of solar heating.

The horizontal kinetic energy in a wavenumber space (per unit mass per unit wavenumber) [17] is analyzed for T159 simulation. The horizontal kinetic energy is decomposed into rotational and divergent components and averaged over the last one year of the integration. Spectra at eight sigma levels are shown in Fig. 3a and b. The rotational component describes the contribution of horizontally balanced flow, such as Rossby waves, to the horizontal kinetic energy in each wavenumber; whereas the divergent one describes that of unbalanced flow such as gravity waves. The spectrum of the rotational component at  $\sigma = 0.03$  ( $\sim 40$  km) shows the  $-3$  power law for  $n < 20$ ; whereas the spectra in the other levels are gentler than the  $-3$  power law but steeper than the  $-5/3$  one. The divergent component in the upper two levels shows the  $-5/3$  power law extending to very small wavenumbers (planetary scales). Further, the ratios of the divergent component to the rotational one for each level are examined. For  $n > 10$ , the divergent component is comparable to rotational component or dominant. The dominance of the divergent component even in the low wavenumbers might be a unique feature of the Venus atmosphere.

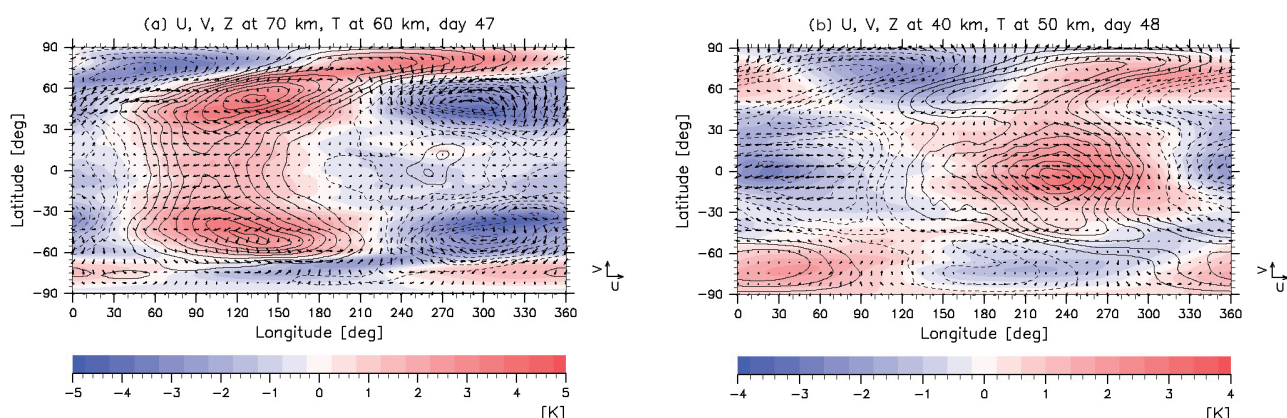


Fig. 1 Horizontal distributions of geopotential height (black contours) and horizontal flow (black vectors) associated with the short-period disturbances at 70 km height, and temperature deviation at 60 km height (color shades) at day 47 (a), and those at 40 km and at 50 km at day 48 (b) from ten Earth years. A band-pass filter between the periods of 2 and 8 Earth days is applied. Contour intervals are 25 m for (a) and 1 m for (b) and vector units are 50 m/s for (a) and 5 m/s for (b), respectively.

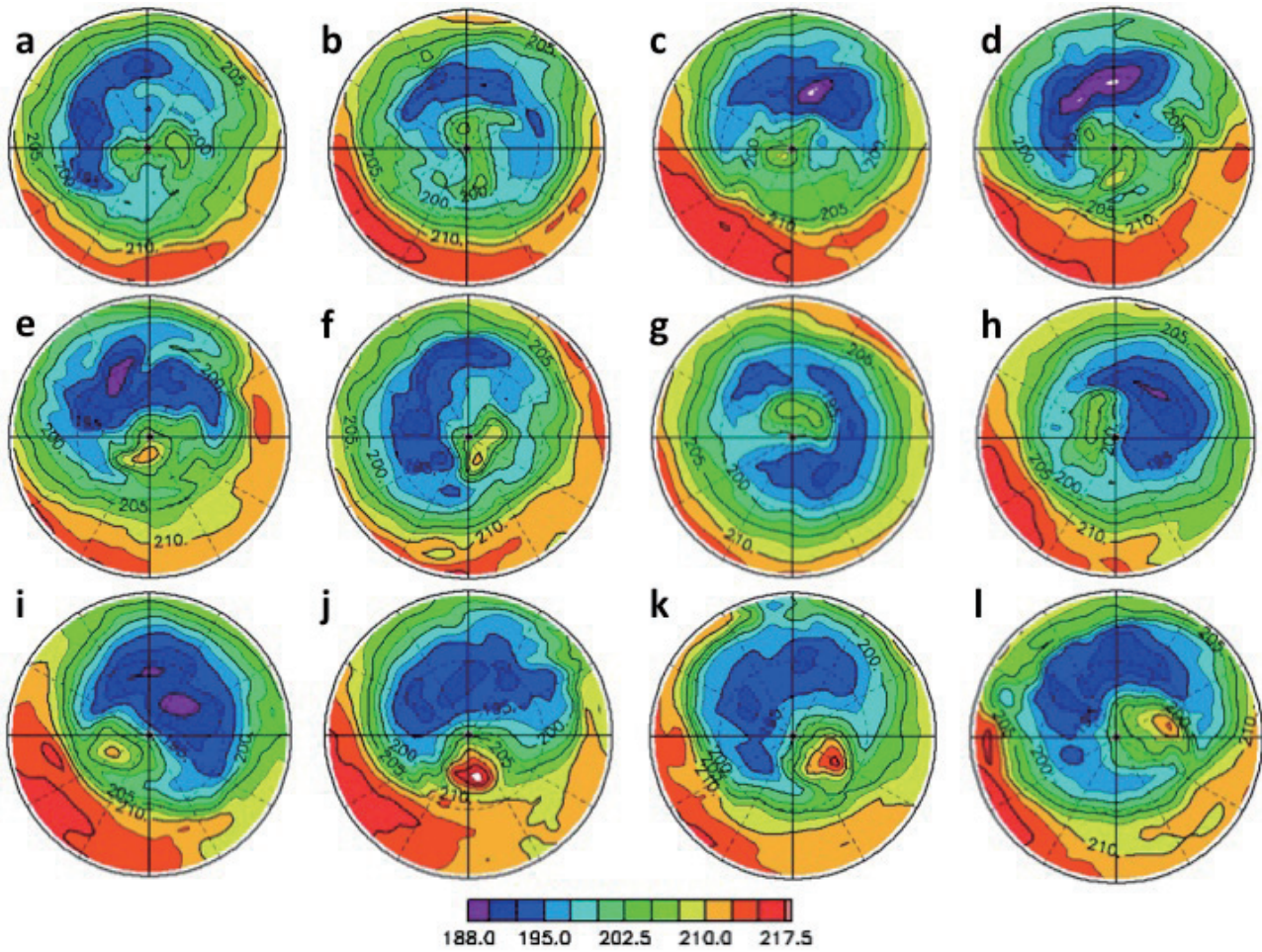


Fig. 2 Time evolution of temperature (K) in the polar plot at the altitude of  $\sim 68$  km. The latitude from  $30^\circ\text{N}$  to  $90^\circ\text{N}$  is shown, and the elapsed time from the start time of the analysis is 681 Earth days. The time interval of respective figures is one Earth day.

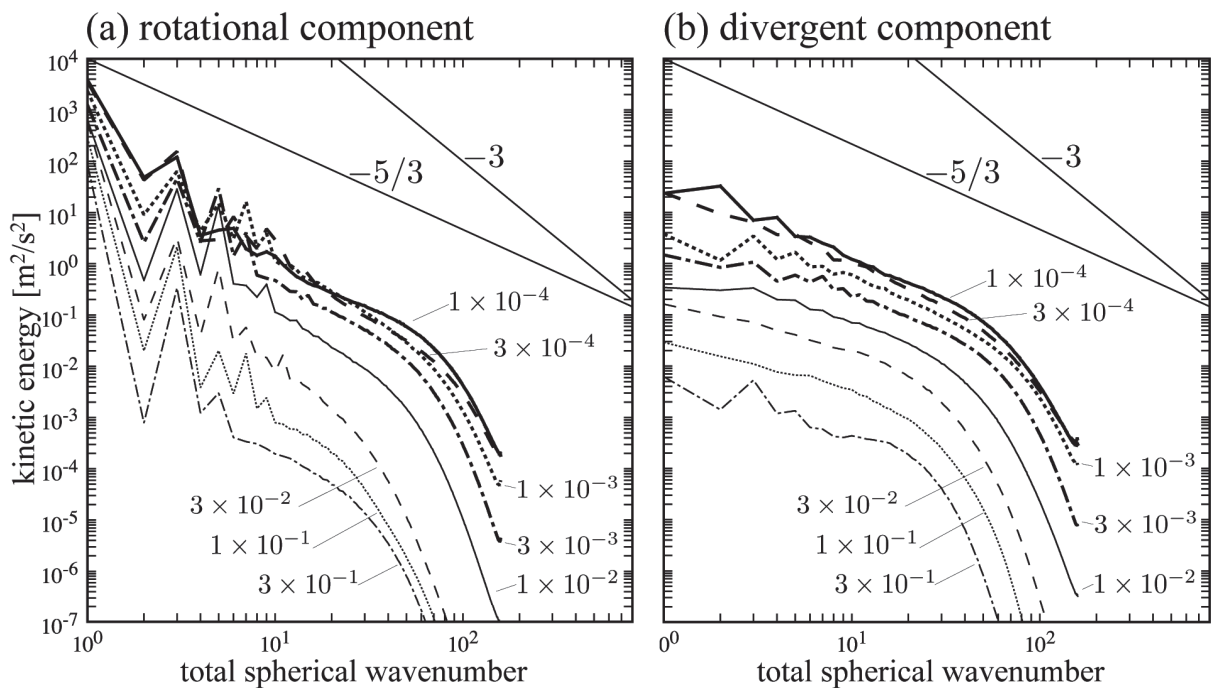


Fig. 3 Horizontal kinetic energy per unit mass per unit wavenumber: (a) rotational component and (b) divergent component. Two straight lines in each panel show slopes of  $-3$  power law and  $-5/3$  power law, respectively.

### 3. Mars simulation

#### 3.1 Targets of simulations

Radiative effect of dust suspended in the Martian atmosphere has important impacts on the thermal and the circulation structures of the Martian atmosphere. However, it has not been well understood what kind of dynamical phenomena contribute to dust lifting from the ground into the atmosphere. A previous study by using a Mars GCM [16] suggests that the effects of subgrid scale wind fluctuations caused by small and medium scale disturbances would be important for the dust lifting processes. However, the features of small and medium scale disturbances which may contribute to dust lifting have not been revealed yet. Disturbances of these scales are not easy to be observed and to be resolved in numerical models. We have been performing medium and high resolution simulations of Martian atmosphere by using our Martian AFES to reveal the features of small and medium scale disturbances in the Martian atmosphere and its effects on dust lifting.

In the preceding fiscal years, our simulations showed that a lot of small scale vortices are generated in the low latitudes. It was also shown that these vortices significantly contribute dust lifting. However, it was not clear how robust these vortices were, because the size of those vortices corresponds roughly to the minimum resolvable scale of the model. It is anticipated that those vortices are generated as a result of thermal convective motion represented in the model, but it may depend on a convective parameterization implemented in the model. In this fiscal year, we examine the nature of these small scale vortices by investigating its dependence on parameterization used in the model.

#### 3.2 Model and experimental settings

Mars simulations are performed with the AFES including physical processes introduced from the Mars GCM [18,19] which has been developed in our group, and with the values of physical constants appropriate for the Mars. The implemented physical processes are radiative, turbulent mixing, and surface processes. With these physical processes, effect of subgrid scale convection is evaluated by the turbulent mixing parameterization based on Mellor and Yamada [20] level 2.5. In this fiscal year, an additional parameterization, convective adjustment, is implemented in the model. The convective adjustment is an extreme of representation of thermal convection, because unstable stratification is not allowed. By the use of this model, several simulations are performed with resolutions of T79L96 and T319L96, which are equivalent to about 44 and 22 km horizontal grid sizes, respectively, and 96 vertical layers. In the simulations, the atmospheric dust distribution is prescribed, and the dust is uniformly distributed in the horizontal direction with an amount corresponding to visible optical depth of 0.2. However, the dust lifting parameterization [21] is included in the model to diagnose the possible amount of dust lifting.

#### 3.3 Results

Figures 4 and 5 show snapshots of distribution of relative vorticity at 4 hPa pressure level from T319L96 simulations without and with convective adjustment. Here, we focus on small scale vortices in the low latitudes. It is shown that the use of convective adjustment does not have an essential effect on existence of small scale vortices. Indeed, the region where the vortices are generated in the simulation with convective adjustment is almost the same as that in the simulation without convective adjustment. However, the strength of vorticity of each vortex is slightly weaker in the simulation with convective adjustment than that in the simulation without convective adjustment.

In order to examine the behavior of the vortices, simulations with uniform surface properties are performed. Flat surface, uniform surface albedo distribution, and uniform soil thermal inertia distribution are used in these simulations. Figures 6 and 7 are the same as Figs. 4 and 5, respectively, except for simulations with the uniform surface properties. In a simulation with uniform surface properties and without convective adjustment, small scale vortices are observed as is the case with non-uniform surface properties. However, the structure of vorticity in the low latitudes in the simulation with the uniform surface properties and with convective adjustment is different

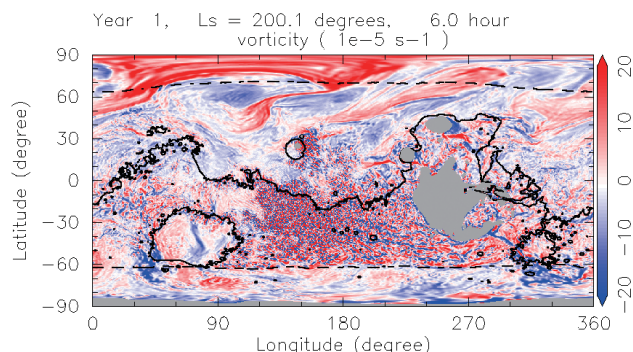


Fig. 4 Global distribution of vorticity at 4 hPa pressure level at northern fall with the resolution of T319L96 without convective adjustment. Unit of vorticity is  $10^{-5} \text{ s}^{-1}$ . Also shown is the areoid (solid line) and low latitude polar cap edge (dashed line). Gray areas represent mountains at the 4 hPa pressure level.

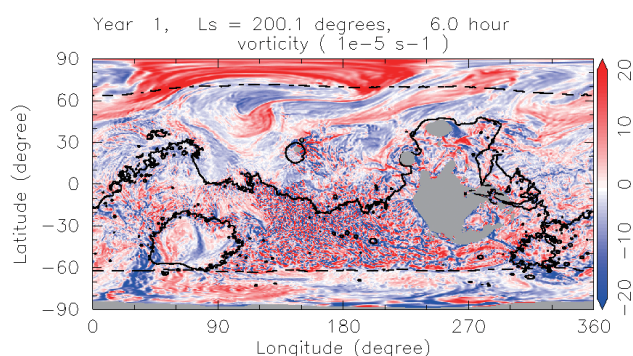


Fig. 5 Same as Fig. 4, but for the simulation with convective adjustment.

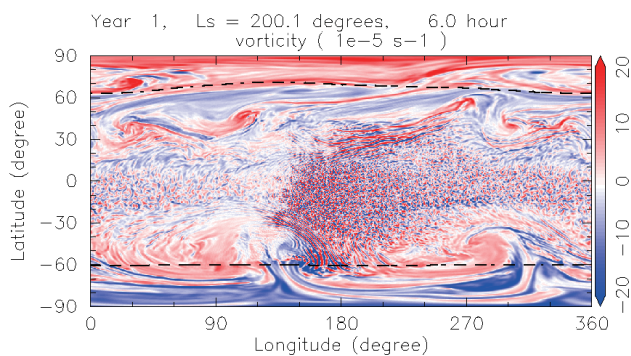


Fig. 6 Same as Fig. 4, but for the simulation with the uniform surface properties.

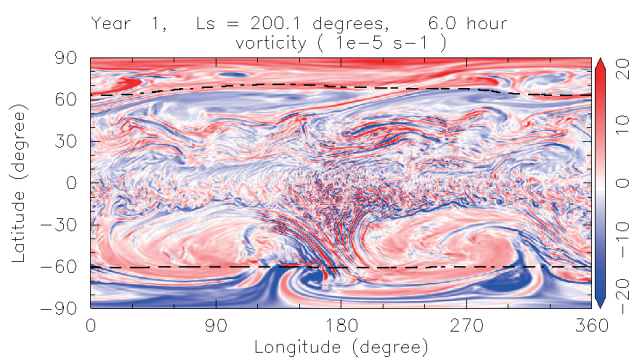


Fig. 7 Same as Fig. 6, but for the simulation with convective adjustment.

from that without convective adjustment. A lot of filaments of vorticity rather than vortices are observed. It is also observed that the filament structures are generated from remnant of vorticity filaments originated from mid-latitude waves.

These results indicate that existence of small scale vortices in the low latitudes does not depend on the details of expression of subgrid scale thermal convection in the model, although the strength of small scale vortices depends on the choice of parameterization. It also implies that the form of small vortices would be plausible in the real atmosphere, since small scale spatial variations of surface properties, such as orographic variation, easily destroy the filament structure, which is observed in the ideal simulation with the uniform surface properties.

## References

[1] Ohfuchi, W., H. Nakamura, M. K. Yoshioka, T. Enomoto, K. Takaya, X. Peng, S. Yamane, T. Nishimura, Y. Kurihara, and K. Ninomiya, "10-km Mesh Meso-scale Resolving Simulations of the Global Atmosphere on the Earth Simulator - Preliminary Outcomes of AFES (AGCM for the Earth Simulator) ", *Journal of the Earth Simulator*, 1, 8, 2004.

[2] Yamamoto, M. and M. Takahashi, "The fully developed superrotation simulated by a general circulation model of a Venus-like atmosphere", *J. Atmos. Sci.*, 60, 561–574, 2003.

[3] Belton, M. J. S., G. R. Smith, G. Schubert, and A. D. Del Genio, "Cloud patterns, waves and convection in the Venus atmosphere", *J. Atmos. Sci.*, 33, 1394–1417, 1976.

[4] Del Genio, A. D. and W. B. Rossow, "Planetary-scale waves and the cyclic nature of cloud top dynamics on Venus", *J. Atmos. Sci.*, 47, 293–318, 1990.

[5] Khatuntsev, I. V., M. V. Patsaeva, D. V. Titov, N. I. Ignatiev, A. V. Turin, S. S. Limaye, W. J. Markiewicz, M. Almeida, T. Roatsch, and R. Moissl, "Cloud level winds from the Venus Express Monitoring Camera imaging", *Icarus*, 226, 140–158, doi:10.1016/j.icarus.2013.05.018, 2013.

[6] Taylor, F. W. et al., "Structure and meteorology of the middle atmosphere of Venus: Infrared remote sensing from the Pioneer Orbiter", *J. Geophys. Res.*, 85, 7963–8006, 1980.

[7] Leroy, S. S. and A. P. Ingersoll, "Radio scintillations in Venus's atmosphere: application of a theory of gravity wave generation", *J. Atmos. Sci.*, 53, 1018–1028, 1996.

[8] Nastrom, G. D. and K. S. Gage, "A climatology of atmospheric wavenumber spectra of wind and temperature observed by commercial aircraft", *J. Atmos. Sci.*, 42, 950–960, 1985.

[9] Takahashi, Y. O., K. Hamilton, and W. Ohfuchi, "Explicit global simulation of the mesoscale spectrum of atmospheric motions", *Geophysical Research Letters*, 33, L12812, doi:10.1029/2006GL026429, 2006.

[10] Sugimoto, N., M. Takagi, Y. Matsuda, Y. O. Takahashi, M. Ishiwatari, and Y.-Y. Hayashi, "Baroclinic modes in the atmosphere on Venus simulated by AFES", *Theoretical and Applied Mechanics Japan*, 61, 11–21, 2013.

[11] Sugimoto, N., M. Takagi, and Y. Matsuda, "Baroclinic instability in the Venus atmosphere simulated by GCM", *J. Geophys. Res., Planets*, 119, 1950–1968, 2014.

[12] Crisp, D., "Radiative forcing of the Venus mesosphere: I. solar fluxes and heating rates", *Icarus*, 67, 484–514, 1986.

[13] Tomasko, M. G., L. R. Doose, P. H. Smith, and A. P. Odell, "Measurements of the flux of sunlight in the atmosphere of Venus", *J. Geophys. Res.*, 85, 8167–8186, 1980.

[14] Gierasch, P. J., R. M. Goody, R. E. Young, D. Crisp, C. Edwards, R. Kahn, D. Rider, A. del Genio, R. Greeley, A. Hou, C. B. Leovy, D. McCleese, and M. Newman, "The General Circulation of the Venus Atmosphere: an Assessment", In *Venus II: Geology, Geophysics, Atmosphere, and Solar Wind Environment*. University of Arizona Press, p.459, 1997.

[15] Hosouchi, M., T. Kouyama, N. Iwagami, S. Ohtsuki, and M. Takagi, "Wave signature in the Venus dayside cloud layer at 58–64 km observed by ground-based infrared spectroscopy", *Icarus*, 220, 552–560, 2012.

[16] Sugimoto, N., M. Takagi, and Y. Matsuda, "Waves in a

- Venus general circulation model”, *Geophysical Research Letters*, 41, 7461–7467, 2014.
- [17] Koshyk, J. N. and K. Hamilton, “The horizontal kinetic energy spectrum and spectral budget simulated by a high-resolution troposphere-stratosphere-mesosphere GCM”, *J. Atmos. Sci.*, 58(4), 329–348, 2001.
- [18] Takahashi, Y. O., H. Fujiwara, H. Fukunishi, M. Odaka, Y.-Y. Hayashi, and S. Watanabe, “Topographically induced north-south asymmetry of the meridional circulation in the Martian atmosphere”, *J. Geophys. Res.*, 108, 5018, doi:10.1029/2001JE001638, 2003.
- [19] Takahashi, Y. O., H. Fujiwara, and H. Fukunishi, “Vertical and latitudinal structure of the migrating diurnal tide in the Martian atmosphere: Numerical investigations”, *J. Geophys. Res.*, 111, E01003, doi:10.1029/2005JE002543, 2006.
- [20] Mellor, G. L. and T. Yamada, “Development of a turbulent closure model for geophysical fluid problems”, *Rev. Geophys. Space Phys.*, 20, 851–875, 1982.
- [21] Newman, C. E., S. R. Lewis, and P. L. Read, “Modeling the Martian dust cycle 1. Representation of dust transport processes”, *J. Geophys. Res.*, 107, 5123, doi:10.1029/2002JE001910, 2002.

## AFES を用いた地球型惑星の大気大循環シミュレーション

課題責任者

林 祥介 神戸大学 大学院理学研究科

著者

林 祥介 神戸大学 大学院理学研究科

高橋 芳幸 神戸大学 大学院理学研究科

杉本 憲彦 慶應義塾大学 自然科学研究教育センター

高木 征弘 京都産業大学 理学部

檜村 博基 海洋研究開発機構 気候変動リスク情報創生プロジェクトチーム

石渡 正樹 北海道大学 大学院理学研究院

小高 正嗣 北海道大学 大学院理学研究院

中島 健介 九州大学 大学院理学研究院

はしもとじょーじ 岡山大学 大学院自然科学研究科

松田 佳久 東京学芸大学 教育学部

大気大循環モデル AFES (AGCM (Atmospheric General Circulation Model) for the Earth Simulator) に基づく GCM を用いて、金星および火星大気の高解像度大気大循環シミュレーションを実施した。我々の研究の目的は、地球型惑星大気における中小規模擾乱の力学的特徴と、その大気大循環への影響を調べることである。金星大気シミュレーションに関しては、観測と整合的なスーパーローテーションが現実的な太陽加熱でうまく再現、維持された。東西風の鉛直シアの大きい低安定度の雲層高度に傾圧波が発生した。雲層上端高度で観測されるいわゆるロスビー波とケルビン波もモデル内に発生した。これらの波は運動量や熱を輸送する。さらに、周極帯状低温域 (cold collar) が極域で再現され、熱潮汐波によって強化された平均子午面循環がその構造と結びついていた。こうした特徴はいずれも観測結果とよく一致している。高解像度計算 (T159L120) では、水平運動エネルギーのスペクトル解析によって、小規模重力波が地球に比べて金星ではより重要である可能性が示唆された。また、モデル中に現れた極渦の構造について、観測と比較した解析を行い、S字構造や鉛直構造が、観測と整合的であることが確認された。これらの結果は、熱潮汐波を含めた現実的な安定度の鉛直分布と十分な解像度が金星大気の大気大循環の再現に必要なことを強く示唆している。火星大気シミュレーションでは、これまでの高解像度計算で見られていた小規模渦の特性を調べるために対流調節過程を導入した付加的な実験を実施した。これまでに行ってきた高解像度計算で見られた最も目立つ大気擾乱の一つは、低緯度における小規模渦であった。しかしながら、それらの構造がどれだけ頑健なものなのかははっきりしておらず、モデルで用いている物理過程に依存する可能性も考えられた。対流調節過程を導入して実施した実験では、わずかに渦の強度が弱くなったものの、やはり小規模渦は生成された。また、それら擾乱のより自然な状態を調べるために、地形やアルベド、熱慣性の空間変化をなくして対流調節過程を導入して行った実験では、渦ではなくフィラメント状の構造が現れた。これらの結果は、小規模渦の存在がモデルで用いているパラメタリゼーションの詳細には依らないこと、そして、それらの渦が地形起源の大気擾乱によって乱されたフィラメント構造から生成されていることを示している。

キーワード: 惑星大気, スーパーローテーション, ダストストーム, 地球, 火星, 金星